



Photocatalytic reduction behavior of hexavalent chromium on hydroxyl modified titanium dioxide



Yali Li¹, Yingying Bian¹, Hongxia Qin, Yaxi Zhang, Zhenfeng Bian^{*}

The Education Ministry Key Lab of Resource Chemistry and Shanghai Key Laboratory of Rare Earth Functional Materials, Shanghai Normal University, Shanghai 200234, PR China

ARTICLE INFO

Article history:

Received 1 December 2016
Received in revised form 12 January 2017
Accepted 17 January 2017
Available online 18 January 2017

Keywords:

Photocatalysis
Titanium dioxide
Hydroxyl modification
Hexavalent chromium reduction

ABSTRACT

The selective adsorption of hexavalent chromium ($\text{Cr}_2\text{O}_7^{2-}$ (Cr(VI))) and the desorption of trivalent chromium (Cr^{3+} (Cr(III))) at the surface of photocatalysts are very important factors in determining the photocatalytic reduction activity of Cr(VI). Here, a homogeneous anchoring of hydroxyl groups on TiO_2 was achieved via a simple soaking method in alkaline solution. The increase of surface hydroxyl groups was confirmed by X-ray photoelectron spectroscopy (XPS) and Fourier transformed infrared spectra (FTIR). Moreover, the zeta potential analysis revealed the positive charged TiO_2 surface in the acid system shown a significant improvement. The surface positive charges had the selective adsorption for Cr(VI) and desorption for Cr(III). Further experimental results revealed that such selective adsorption process played important roles in the photocatalytic reduction of Cr(VI). Finally, a process of selective adsorption/desorption promoted photocatalytic reduction of Cr(IV) was proposed in detail.

© 2017 Elsevier B.V. All rights reserved.

1. Introduction

Hexavalent chromium (Cr(VI)) from industrial activities (such as electroplating, metal finishing, leather tanning, steel fabricating, photographic, etc.) discharged into water body and resulted in serious environmental pollution [1,2]. Unfortunately, Cr(VI) is known to be mutagenic, carcinogenic and toxic substance, which is harmful to biological systems and can easily enter the food chains [3,4]. Maximum permissible concentration of Cr(VI) in drinking water is 0.05 mg/L [5]. Therefore, it is crucial importance to remove Cr(VI) from wastewater. Many researchers have been done some efforts. The conventional methodologies of removing Cr(VI) such as ion exchange, bioremediation, membrane separation and adsorption or chemical precipitation suffered from limitations like sludge generation, incomplete precipitation, high operating cost, etc [6–9]. Activated carbon, for example, is widely used for the absorption of Cr(VI) [9]. However, the problem is that it can only be used for adsorption of Cr (VI) and desorption of Cr (VI) still needed other treatment. One of the most preferred methods to treat Cr(VI) in wastewater is the transformation of Cr(VI) to Cr(III) [10]. The Cr(III) is considered to be nontoxic and is an essential trace metal in human nutrition [11]. In addition, it can be precipitated out of solu-

tion in the form of $\text{Cr}(\text{OH})_3$ and removed as a solid waste [12]. Therefore, the reduction of Cr(VI) to Cr(III) is regarded as a key process for the treatment of wastewater containing Cr(VI).

Many alternative processes such as chemical reduction and photo-reduction have been proposed for the reduction of Cr(VI) [13,14]. Among these methods, photocatalysis is a promising technique since it achieves the one-step removal of Cr(VI) by utilizing sunlight. TiO_2 , owing to its stability, low cost, and nontoxicity properties, is one of the most important semiconductors being commonly used in heterogeneous photocatalysis [15–21]. It has been reported that TiO_2 can photocatalytic reduce Cr(VI) to Cr(III) where it serves as an electron donor during the reduction of Cr (VI) to Cr (III) [14,22,23].

The photocatalytic reduction activity of TiO_2 is strongly dependent on the interfacial reaction. When Cr(VI) is photocatalytic reduced, it should first adsorb on the surface of TiO_2 . Photogenerated electrons migrate to TiO_2 surfaces and react with Cr(VI). As the Cr(VI) is reduced to Cr(III), the Cr(III) is quickly removed from the surface. This completes the photocatalytic reduction process. Many efforts have been devoted to improve the adsorption capacity and photocatalytic activity of TiO_2 nanomaterials by various strategies, including designing the porous structure to increase specific surface area, combining with adsorbent to improve the adsorption performance, metal or nonmetal doping or modifying with noble metals to promote charge separation [13–15,22–25]. However, increasing specific surface area or combining with adsorbent

* Corresponding author.

E-mail addresses: bianzhenfeng@163.com, bianzhenfeng@shnu.edu.cn (Z. Bian).

¹ Equal contribution as the first author.

focuses on the adsorption performance. In order to efficiently utilize the photocatalytic performance, it is necessary to develop the surface adsorption of Cr(VI) as well as repulsion of Cr(III). However, to the best of our knowledge, no attention has ever been paid to study it.

Herein we report that the hydroxyl group modified TiO_2 was prepared by a simple soaking method in alkaline solution, which was used for photocatalytic reduction of aqueous Cr(VI). The results showed that it can significantly improve the selective adsorption of Cr(VI) as well as desorption of Cr(III). The selectivity greatly improved the performance of the photocatalytic reduction of Cr(VI). The photocatalytic performance on the photocatalytic reduction of Cr(VI) to Cr(III) was investigated in detail, including the concentration of hydroxyl groups, the stability of the catalyst, and the photocatalytic reduction mechanism was also proposed. It is expected that our current work could provide guided information for design and fabricate efficient photoactive materials for photocatalytic reduction of Cr(VI).

2. Experiment section

2.1. Chemicals and materials

TiOSO_4 (15 wt% solution in dilute sulfuric acid, purchased from Sigma-Aldrich) and tert-butyl alcohol, ethanol, NaOH, $\text{K}_2\text{Cr}_2\text{O}_7$, $\text{Cr}(\text{NO}_3)_3 \cdot 9\text{H}_2\text{O}$, HCl, Diphenylcarbazide were purchased from aladdin (AR, Shanghai, China). All the chemicals were used as received. Commercial P25 (TiO_2 , Degussa) and ST21 (TiO_2 , Ishihara Sangyo) were used as received.

2.2. Preparation of the TiO_2 photocatalysts and surface modification

As-prepared TiO_2 were prepared by an alcoholysis route according to our previous work [26]. In a typical synthesis, 2.0 mL TiOSO_4 was slowly added into 40 mL tert-butyl alcohol. The mixture was transferred into a 50 mL Teflon-lined autoclave (48 h, 110 °C). The product was filtered, washed thoroughly with ethanol. The product was subsequently calcined in air (5°C min^{-1}) at 350 °C for 120 min. The prepared sample was named MT (Mesocrystals TiO_2). Hydroxyl group modified TiO_2 were synthesized by a soaking method in alkaline solutions. 0.5 g TiO_2 (MT, P25, ST21) was slowly added to 50 mL (0.5, 1.0, 2.0 mol/L) NaOH solution and stirred for 0.5 h. Then, the product was washed thoroughly to neutral by deionized water, and finally vacuum drying for 24 h. The prepared sample was named MT (P25, ST21)-x ($x = 0.5, 1.0, 2.0$), in which x represented the amounts of NaOH solution.

2.3. Characterization

The TiO_2 morphology was characterized by scanning electron microscopy (SEM, HITACHI S4800). The photocatalyst structure was characterized using X-ray diffraction (XRD, D/MAX-2000 with

$\text{Cu K}\alpha$ radiation), Fourier transformation infrared spectrum (FTIR, NEXUS 370) and nitrogen sorption (Micromeritics Instrument Corporation, Tristar II 3020, at 77 K). The Brunauer-Emmett-Teller (BET) method was utilized to calculate the specific surface area. The pore volume and pore diameter distribution were derived from the adsorption isotherms by the Barrett-Joyner-Halenda (BJH) model. The pH value was measured with a pH meter (Mettler Toledo Delta 320). Surface electronic states were analyzed by X-ray photoelectron spectroscopy (XPS, PerkinElmer PHI 5000C, Al $\text{K}\alpha$). All the binding energies were calibrated by using the contaminant carbon (C1S = 284.6 eV) as a reference. Zeta potential of the TiO_2 were measured by "Malvern Zetasizer Nano ZS".

2.4. Activity test

2.4.1. Adsorption experiment

In briefly, 20 mg catalyst was added to 20 mL mixture chromium solution (The initial concentration of $\text{Cr}_2\text{O}_7^{2-}$ ions and Cr^{3+} ions in the mixture solution was 10 mg L^{-1}). The mixture was stirred for 0.5 h under the dark condition to reach adsorption–desorption equilibrium. The Cr(VI) concentration was determined by colorimetrically at 540 nm using the diphenylcarbazide method using a UV-vis spectrophotometer (UV 7502/PC) [27]. The amounts of total chromium were determined by inductively coupled plasma (ICP) emission spectroscopy (VISTA-MPX). The concentration of Cr(III) is equal to the total chromium subtracting the Cr(VI) concentration ($\text{Cr(III)} = \text{Cr}_{\text{total}} - \text{Cr(VI)}$).

2.4.2. Photocatalytic reduction

For typical photocatalytic runs, 50 mL of TiO_2 dispersion (1.0 g/L) containing aqueous solution (Cr(VI), 10 mg/L, pH is about 3 controlled by HCl) using a home-made reactor was stirred for about 30 min to reach adsorption–desorption equilibrium in the dark [28,29]. The photocatalytic reaction was initiated by a LED light (CEL-LED, 365 nm). After stopping the UV illumination, the concentration of Cr(VI) was analyzed by a UV spectrophotometer (UV 7502/PC) at the characteristic wavelength, from which the degradation yield was calculated.

3. Results and discussions

The photocatalytic activity of TiO_2 is strongly dependent on the interfacial reaction. For example, the reduction of Cr(VI) requires three steps, adsorption on surface active sites, photo-reduction and surface desorption process, respectively (Fig. 1). Based on the features of the opposite charge properties of Cr(VI) and Cr(III), if the TiO_2 surface has more positive charge, the selective adsorption of Cr(VI) and desorption of Cr(III) should improve the photocatalytic performance. The TiO_2 surface positive charge density can be increased by increasing the surface hydroxyl groups under the acid

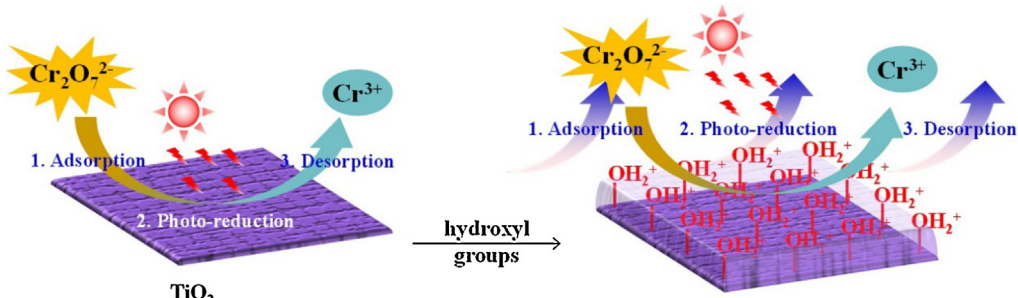


Fig. 1. The process of photocatalytic reduction of Cr(VI) on TiO_2 surface.

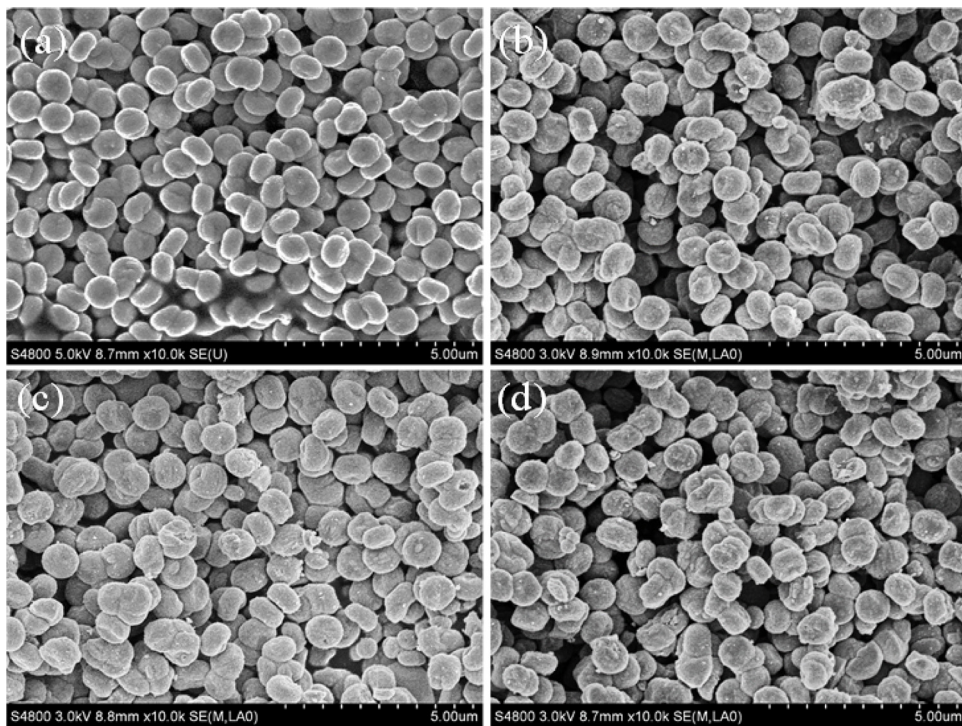


Fig. 2. SEM images of different samples. (a) MT, (b) MT-0.5, (c) MT-1.0, (d) MT-2.0.

reaction conditions. The hydroxyl groups were produced on the surface of TiO_2 via a simple soaking method in alkaline solutions.

Scanning electron microscopy (SEM) was used to examine the structural changes of the as-prepared and alkali treated TiO_2 samples. The TiO_2 samples (named as MT (Mesocrystals TiO_2)) were prepared by an alcoholysis route according to our previous work which possessed a high specific surface area [26]. The SEM images demonstrated that uniform microspheres with average diameter around 600 nm (Fig. 2a). After treating by alkali soaking, there are no apparent change in morphology for MT samples (Fig. 2b–d).

As Fig. 3 shown, all of the TiO_2 samples have well-defined diffraction peaks characteristic of anatase titania structure (JCPDS 21-1272) [29,30]. After the alkali soaking treatment, there were no significant impurity peaks observed, implying that the influence of the mild modification process on the crystal phase structure and crystallinity can be neglected.

The specific surface area (S_{BET}) and the cumulative pore volume (V_p) of the as-prepared MT sample have been measured to be $129 \text{ m}^2 \text{ g}^{-1}$ and $0.10 \text{ cm}^3 \text{ g}^{-1}$, respectively (shown in Table 1). The pore size distribution exhibited a narrow pore size of 3.1 nm. Fig. 4 demonstrated that all the MT samples displayed the similar pore

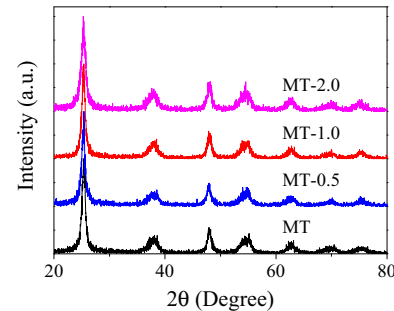


Fig. 3. X-ray diffraction (XRD) patterns of different MT samples.

sizes. It is seen that the texture properties of the MT-0.5, MT-1.0 and MT-2.0 is higher than that of the as-prepared MT sample and S_{BET} slightly increases from 129 to $154 \text{ m}^2 \text{ g}^{-1}$, as well as V_p slightly enhanced from 0.10 to $0.13 \text{ cm}^3 \text{ g}^{-1}$, while the pore size distribution remain unchanged. Such slightly changes might be due to the alkali washing process open some of the block pores in MT sample which results in the increasing of the surface area and pore volume.

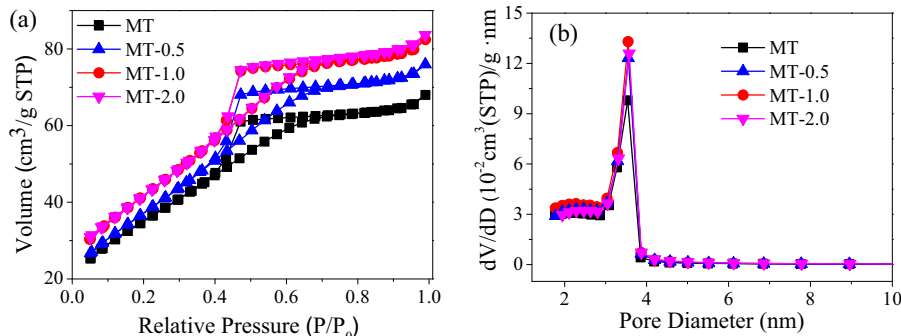
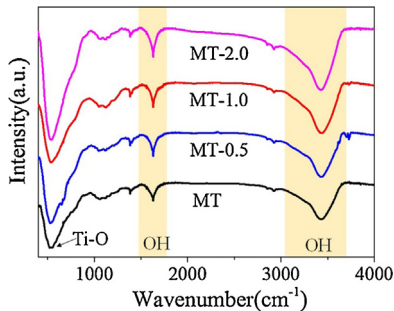


Fig. 4. N_2 adsorption-desorption isotherms (a) and pore size distribution curves (b) of different MT samples.

Table 1

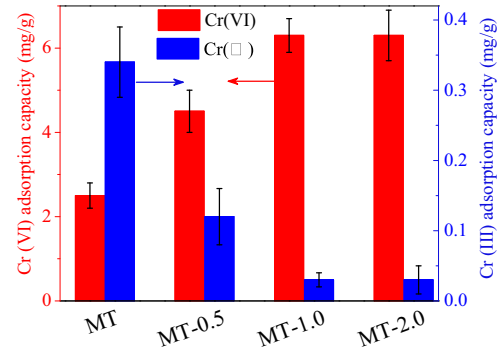
Texture properties and the ratio of Cr(VI)/Cr(III) adsorption capacity of the different MT samples.

Samples	BET Surface Area(m ² /g)	Volume of pores(cm ³ /g)	Average pore diameter(nm)	Ratio of Cr(VI)/Cr(III) adsorption capacity ^a
MT	129	0.10	3.1	7.4
MT-0.5	138	0.12	3.1	37.5
MT-1.0	153	0.13	3.1	200
MT-2.0	154	0.13	3.1	200

^a The adsorption capacity of Cr(VI)/the adsorption capacity of Cr(III).**Fig. 5.** FTIR spectra of the different MT samples.

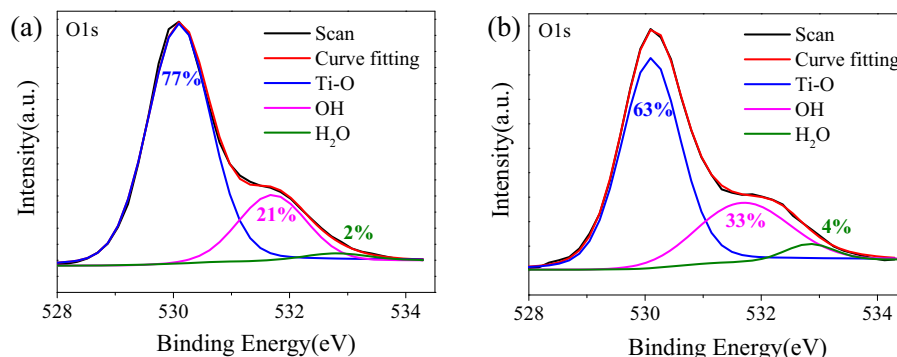
FTIR spectra (Fig. 5) has been employed to detect the hydroxyl groups on TiO_2 surface. A broad stretching vibration near 3400 cm^{-1} and another peak around 1630 cm^{-1} can be attributed to the surface-adsorbed water and hydroxyl groups [31,32], respectively, which become more obvious after alkali soaking treatment. Moreover, XPS was used to investigate the amount of surface hydroxyl groups. According to the literature, there are mainly three kinds of oxygen species on the surface of TiO_2 , such as lattice oxygen, hydroxyl groups and adsorbed H_2O [33]. In order to get reliable data and facilitate comparison, the O1s peak is fitting by pseudo-Voigt functions. In Fig. 6, the O1s signal shows three peaks at 530.1, 531.7 and 532.9 eV. The main peak at 530.1 eV could be ascribed to lattice oxygen in TiO_2 , as well as the signal at 531.7 eV could be associated to surface hydroxyl groups, while the peak at 532.9 eV might be adsorbed H_2O . From the results, it can be seen that the number of surface hydroxyl groups on TiO_2 are significantly improved after alkali soaking, which further confirms the hydroxyl group modification on MT is consistent with the FTIR results.

The selective adsorption experiment was performed on different MT materials. The adsorption of MT to Cr(VI) was 2.5 mg/g and Cr(III) was 0.34 mg/g, respectively. With the number of hydroxyl groups increasing on the surface of MT sample, the adsorption of Cr(III) decreased while the adsorption amount of Cr(VI) increased gradually. The sample of MT-1.0 and MT-2.0 showed priority for Cr(VI) adsorption (6.0 mg/g) while Cr(III) was hardly adsorbed

**Fig. 7.** Adsorption capacities for Cr(VI)/Cr(III) on different MT samples in a mixed solution containing Cr(VI) and Cr(III).

(0.03 mg/g) (Fig. 7). The ratio of Cr(VI)/Cr(III) adsorption capacity increased from 7.4 of MT sample to 200 of MT-1.0 and MT-2.0 samples (Table 1). Therefore, the above results clearly indicate that the presence of hydroxyl groups facilitates the selective adsorption of Cr(VI).

Fig. 8a compared the process of Cr(VI) anions reduction under UV light irradiation. The photocatalytic reduction performance of Cr(VI) anions showed that the MT-1.0 and MT-2.0 were more efficient than the case of pristine MT. The Cr(VI) reduction efficiency decreased from 93% (MT-1.0 and MT-2.0) to 75% (MT) after 30 min of UV irradiation (Fig. 8a). The photocatalytic performance was in good agreement with the number of hydroxyl groups on the surface of MT samples. The reduction of Cr(VI) anions was also described by a pseudo-first-order reaction expression with a simplified Langmuir–Hinshelwood model. The rate of photocatalytic reduction was calculated to be 0.044 min^{-1} for MT, which was lower than that of MT-1.0 and MT-2.0 (about 0.079 min^{-1} , Fig. 8b). The enhancements of about 80% in the rate was observed after modified with hydroxyl groups on the surface of MT materials. Excluding the influence of the specific surface area, the performance is increased about 70%. Based on the above results, MT-1.0 and MT-2.0 have the similar results which might be due to the saturation of surface hydroxyl modification. Therefore, we opti-

**Fig. 6.** XPS spectra of (a) MT and (b) MT-1.0 sample.

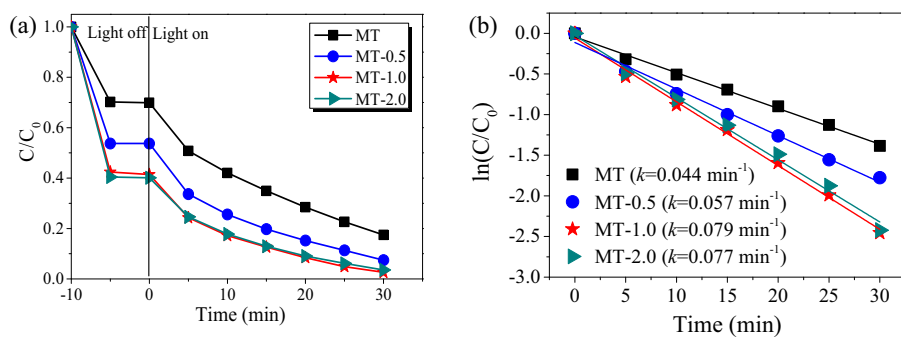


Fig. 8. Liquid-phase photocatalytic Cr(VI) anion reduction (a) and kinetic linear fitting curves (b) on different TiO_2 samples. ($\text{pH} = 3.0$; $\ln(C_0/C_t) = kt$, where C_t is the concentration of organics at time t , and k is the apparent first-order rate constant.) [34].

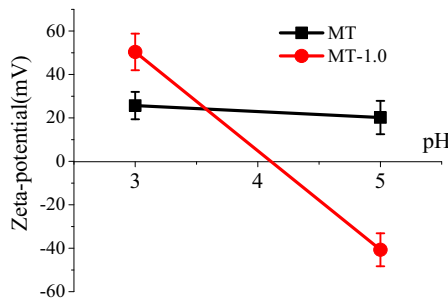


Fig. 9. Zeta potentials of MT and MT-1.0 samples.

maximized the concentration of NaOH solution about 1.0 mol/L for alkali soaking.

Zeta-potential of MT and MT-1.0 samples were measured to confirm the surface charge properties (Fig. 9). A more positive zeta-potential value was observed for the MT-1.0 sample (50.4 mV) in comparison with pristine MT (25.7 mV) when pH was 3.0. A more positive charge surface was beneficial to the process of Cr(VI) absorption and Cr(III) desorption in the photocatalytic reduction process. However, when the pH was 5, the zeta-potential value was diametrically opposed. The MT-1.0 sample was about -40 mV and MT sample was about 20 mV. Reduction ability of MT-1.0 was only achieved 44% and the reduction rate was about 0.017 min^{-1} at pH 5 which is lower than that of MT (Fig. 10). The above results indicate that the photocatalytic reduction performance of MT and MT-1.0 was completely changed at pH 5, which proved the decisive role of selective adsorption-desorption of the chromium ion on the photocatalytic reduction performance.

The durability and stability is an important aspect for evaluating the photocatalytic reduction of TiO_2 . As shown in Fig. 11, the MT-1.0 sample retained 40% yield after 5 times photocatalytic reduction of

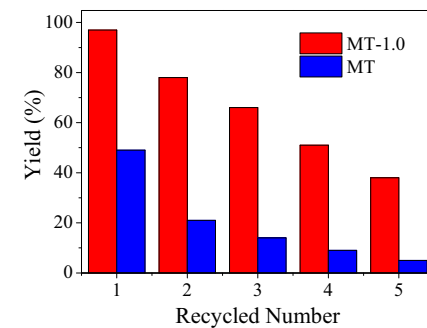


Fig. 11. Recycling tests of the MT and MT-1.0 samples. ($\text{pH} = 3.0$).

Cr(VI), while the pristine MT retained only 5% (almost inactivation) yield after 5 times reaction. The relative higher durability of MT-1.0 should be attributed to the plenty of surface positive charge on MT-1.0 which is benefit to remove Cr(III) cation without metal ion poison. On the contrary, the deactivation of pristine MT should be the slow release of Cr(III) cation and coverage on the active site of TiO_2 surface for efficient photocatalytic reduction.

This principle can be extended to other semiconductor photocatalysts in photocatalytic reduction of ionic pollutants with varied charges. For example, using commercial titania P25 and ST21 as raw materials, we prepared the P25-1.0 and ST21-1.0 samples. As shown in Fig. 12, the photocatalytic performance of Cr(VI) anion reduction on P25-1.0 and ST21-1.0 samples are significantly improved in comparison with the pristine one. Accordingly, the precise control of surface functional groups to adjusting the surface charges can effectively realize the selective adsorption/desorption of Cr(VI)/Cr(III) ions, and thus the photocatalytic reduction performance can be improved.

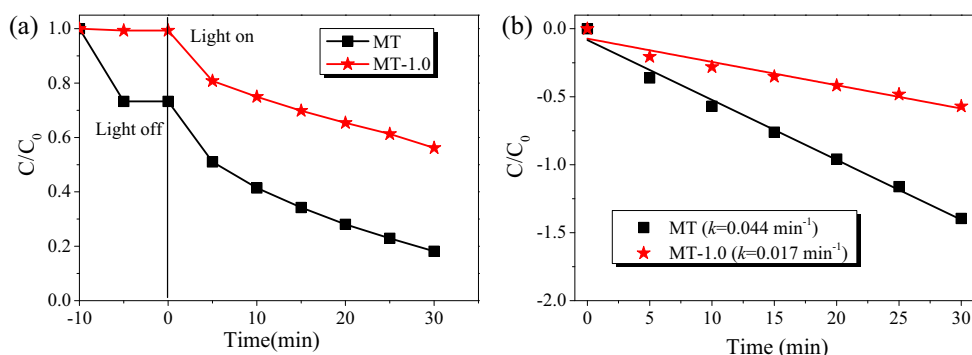


Fig. 10. Liquid-phase photocatalytic Cr(VI) anion reduction (a) and kinetic linear fitting curves (b) on MT and MT-1.0 sample at pH 5.0.

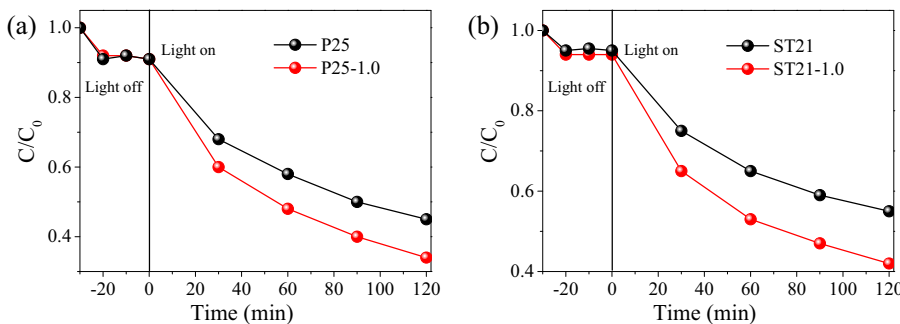


Fig. 12. Liquid-phase photocatalytic Cr(VI) anion reduction of (a) P25, P25-1.0 and (b) ST21, ST21-1.0 at pH 3.0.

4. Conclusion

In summary, the photocatalytic reduction of Cr(VI) to Cr(III) was more efficient on hydroxyl groups modified TiO_2 by a simple alkali soaking method. The TiO_2 surface possessed high positive charge under the acidic system when the surface was modified by hydroxyl groups. The selective adsorption of Cr(VI) and the desorption of Cr(III) was present. Therefore, the pH value of the reaction solution is crucial to the selective adsorption of Cr(VI) and desorption of Cr(III) on the hydroxyl modified TiO_2 surface. The proposed principle can also extend to commercial TiO_2 photocatalysts to improve their photocatalytic reduction performances. With the hydroxyl groups, TiO_2 based photocatalysts possessed higher durability owing to the fast release of Cr(III) product and relief the coverage on active sites. This easily handled and efficient strategy paves the way for hydroxyl group modified semiconductor photocatalysts to enhance the photocatalytic reduction activity and durability of Cr(VI). It is expected that our current work could provide a simple and effective way in photocatalytic reduction of ionic pollutants.

Acknowledgments

This work is supported by National Natural Science Foundation of China (21237003, 21407106, 21522703, 21377088), Shanghai Government (14ZR1430800, 13SG44, 15520711300), and International Joint Laboratory on Resource Chemistry (IJLRC). Research is also supported by The Program for Professor of Special Appointment (Eastern Scholar) at Shanghai Institutions of Higher Learning and Shuguang Research Program of Shanghai Education Committee.

References

- S. Babel, T.A. Kurniawan, Cr(VI) removal from synthetic wastewater using coconut shell charcoal and commercial activated carbon modified with oxidizing agents and/or chitosan, *Chemosphere* 54 (2004) 951–967.
- S. Congeeveraram, S. Dhanarani, J. Park, M. Dexilin, K. Thamaraiselvi, Biosorption of chromium and nickel by heavy metal resistant fungal and bacterial isolates, *J. Hazard. Mater.* 146 (2007) 270–277.
- A. Linos, A. Petralias, C.A. Christophi, E. Christoforidou, P. Kouroutou, M. Stoltidis, A. Veloudaki, E. Tzala, K.C. Makris, M.R. Karagas, Oral ingestion of hexavalent chromium through drinking water and cancer mortality in an industrial area of Greece—an ecological study, *Environ. Health Perspect.* 120 (2012) 50.
- C.M. Thompson, D.M. Proctor, L.C. Haws, C.D. Hebert, S.D. Grimes, H.G. Shertzer, A.K. Kopec, J.G. Hixon, T.R. Zacharewski, M.A. Harris, Investigation of the mode of action underlying the tumorigenic response induced in B6C3F1 mice exposed orally to hexavalent chromium, *Toxicol. Sci.* 123 (2011) 58–70.
- A. Zhitkovich, Chromium in drinking water: sources, metabolism, and cancer risks, *Chem. Res. Toxicol.* 24 (2011) 1617–1629.
- A. Dabrowski, Z. Hubicki, P. Podkoscilny, E. Robens, Selective removal of the heavy metal ions from waters and industrial wastewaters by ion-exchange method, *Chemosphere* 56 (2004) 91–106.
- U. Badar, N. Ahmed, A.J. Beswick, P. Pattanapipitpaisal, L.E. Macaskie, Reduction of chromate by microorganisms isolated from metal contaminated sites of Karachi Pakistan, *Biotechnol. Lett.* 22 (2000) 829–836.
- R. Guell, E. Antico, V. Salvado, C. Fontas, Efficient hollow fiber supported liquid membrane system for the removal and preconcentration of Cr(VI) at trace levels, *Sep. Purif. Technol.* 62 (2008) 389–393.
- D. Mohan, C.U. Pittman Jr., Activated carbons and low cost adsorbents for remediation of tri- and hexavalent chromium from water, *J. Hazard. Mater.* 137 (2006) 762–811.
- Z. Chen, Z. Huang, Y. Cheng, D. Pan, X. Pan, M. Yu, Z. Pan, Z. Lin, X. Guan, Z. Wu, Cr(VI) uptake mechanism of *Bacillus cereus*, *Chemosphere* 87 (2012) 211–216.
- D. Park, Y.-S. Yun, J.M. Park, Reduction of hexavalent chromium with the brown seaweed *ekkonia* biomass, *Environ. Sci. Technol.* 38 (2004) 4860–4864.
- P. Miretzky, A.F. Cirelli, Cr(VI) and Cr(III) removal from aqueous solution by raw and modified lignocellulosic materials: a review, *J. Hazard. Mater.* 180 (2010) 1–19.
- L. Yang, Y. Xiao, S. Liu, Y. Li, Q. Cai, S. Luo, G. Zeng, Photocatalytic reduction of Cr(VI) on WO_3 doped long TiO_2 nanotube arrays in the presence of citric acid, *Appl. Catal. B* 94 (2010) 142–149.
- Y. Zhang, Z. Chen, S. Liu, Y.-J. Xu, Size effect induced activity enhancement and anti-photocorrosion of reduced graphene oxide/ZnO composites for degradation of organic dyes and reduction of Cr(VI) in water, *Appl. Catal. B* 140–141 (2013) 598–607.
- K. Sridharan, E. Jang, T.J. Park, Novel visible light active graphitic $\text{C}_3\text{N}_4\text{-TiO}_2$ composite photocatalyst: synergistic synthesis, growth and photocatalytic treatment of hazardous pollutants, *Appl. Catal. B* 142–143 (2013) 718–728.
- Z. Bian, F. Cao, J. Zhu, H. Li, Plant uptake-assisted round-the-clock photocatalysis for complete purification of aquaculture wastewater using sunlight, *Environ. Sci. Technol.* 49 (2015) 2418–2424.
- Z. Bian, J. Zhu, H. Li, Solvothermal alcoholytic synthesis of hierarchical TiO_2 with enhanced activity in environmental and energy photocatalysis, *Photochem. Photobiol. C* 28 (2016) 72–86.
- F. Cao, Y. Li, C. Tang, X. Qian, Z. Bian, Fast synthesis of anatase TiO_2 single crystals by a facile solid-state method, *Res. Chem. Intermed.* 42 (2016) 5975–5981.
- F. Chen, F. Cao, H. Li, Z. Bian, Exploring the important role of nanocrystals orientation in TiO_2 superstructure on photocatalytic performances, *Langmuir* 31 (2015) 3494–3499.
- X. Li, J. Wang, Y. Men, Z. Bian, TiO_2 mesocrystal with exposed (001) facets and CdS quantum dots as an active visible photocatalyst for selective oxidation reactions, *Appl. Catal. B* 187 (2016) 115–121.
- C. Tang, L. Liu, Y. Li, Z. Bian, Aerosol spray assisted assembly of TiO_2 mesocrystals into hierarchical hollow microspheres with enhanced photocatalytic performance, *Appl. Catal. B* 201 (2017) 41–47.
- R. Mu, Z. Xu, L. Li, Y. Shao, H. Wan, S. Zheng, On the photocatalytic properties of elongated TiO_2 nanoparticles for phenol degradation and Cr(VI) reduction, *J. Hazard. Mater.* 176 (2010) 495–502.
- Y.C. Zhang, J. Li, H.Y. Xu, One-step in situ solvothermal synthesis of $\text{SnS}_2\text{/TiO}_2$ nanocomposites with high performance in visible light-driven photocatalytic reduction of aqueous Cr(VI), *Appl. Catal. B* 123–124 (2012) 18–26.
- X. Liu, L. Pan, Q. Zhao, T. Lv, G. Zhu, T. Chen, T. Lu, Z. Sun, C. Sun, UV-assisted photocatalytic synthesis of ZnO-reduced graphene oxide composites with enhanced photocatalytic activity in reduction of Cr(VI), *Chem. Eng. J. (Amst. Neth.)* 183 (2012) 238–243.
- N. Wang, L. Zhu, K. Deng, Y. She, Y. Yu, H. Tang, Visible light photocatalytic reduction of Cr(VI) on TiO_2 in situ modified with small molecular weight organic acids, *Appl. Catal. B* 95 (2010) 400–407.
- Z. Bian, J. Zhu, J. Wen, F. Cao, Y. Huo, X. Qian, Y. Cao, M. Shen, H. Li, Y. Lu, Single-crystal-like titania mesocages, *Angew. Chem. Int. Ed.* 50 (2011) 1105–1108.
- L. Huang, C.H. Yu, P.K. Hopke, P.J. Liou, B.T. Buckley, J.Y. Shin, Z. Fan, Measurement of soluble and total hexavalent chromium in the ambient airborne particles in New Jersey, *Aerosol Air Qual. Res.* 14 (2014) 1939–1949.
- Z. Bian, T. Tachikawa, T. Majima, Superstructure of TiO_2 crystalline nanoparticles yields effective conduction pathways for photogenerated charges, *J. Phys. Chem. Lett.* 3 (2012) 1422–1427.
- H. Li, Z. Bian, J. Zhu, Y. Huo, H. Li, Y. Lu, Mesoporous Au/TiO₂ nanocomposites with enhanced photocatalytic activity, *J. Am. Chem. Soc.* 129 (2007) 4538–4539.

[30] H. Li, Z. Bian, J. Zhu, D. Zhang, G. Li, Y. Huo, H. Li, Y. Lu, Mesoporous titania spheres with tunable chamber structure and enhanced photocatalytic activity, *J. Am. Chem. Soc.* 129 (2007) 8406–8407.

[31] C. Deiana, E. Fois, S. Coluccia, G. Martra, Surface structure of TiO_2 P25 nanoparticles: infrared study of hydroxy groups on coordinative defect sites, *J. Phys. Chem. C* 114 (2010) 21531–21538.

[32] A. Sharma, B.P. Singh, S. Dhar, A. Gondorf, M. Spasova, Effect of surface groups on the luminescence property of ZnO nanoparticles synthesized by sol-gel route, *Surf. Sci.* 606 (2012) L13–L17.

[33] J. Zhu, J. Yang, Z.-F. Bian, J. Ren, Y.-M. Liu, Y. Cao, H.-X. Li, H.-Y. He, K.-N. Fan, Nanocrystalline anatase TiO_2 photocatalysts prepared via a facile low temperature nonhydrolytic sol-gel reaction of TiCl_4 and benzyl alcohol, *Appl. Catal. B* 76 (2007) 82–91.

[34] Z. Bian, T. Tachikawa, W. Kim, W. Choi, T. Majima, Superior electron transport and photocatalytic abilities of metal-nanoparticle-loaded TiO_2 superstructures, *J. Phys. Chem. C* 116 (2012) 25444–25453.